IEEE Access
Multidisciplinary ⋮ Rapid Review ⋮ Open Access Journal

Received 14 March 2023, accepted 16 May 2023, date of publication 25 May 2023, date of current version 3 July 2023.

Digital Object Identifier 10.1109/ACCESS.2023.3280128

APPLIED RESEARCH

IEC 61850-Based Protection Scheme for Multiple Feeder Faults and Hardware-in-the-Loop Platform for Interoperability Testing

THANAKORN PENTHONG[1], MIRKO GINOCCHI[1], (Member, IEEE), AMIR AHMADIFAR[1], (Member, IEEE), FERDINANDA PONCI[1], (Senior Member, IEEE), AND ANTONELLO MONTI[1,2], (Senior Member, IEEE)

[1]Institute for Automation of Complex Power Systems, RWTH Aachen University, 52074 Aachen, Germany
[2]Fraunhofer-Institut für Angewandte Informationstechnik (FIT), 52062 Aachen, Germany

Corresponding author: Thanakorn Penthong (thanakorn.penthong@eonerc.rwth-aachen.de)

This work was supported by the Interoperability Network for the Energy Transition (IntNET) which is a European Project funded by the European Union's Horizon 2020 Research and Innovation Program under Grant 101070086.

ABSTRACT The existing Overcurrent Protection Function (OCPF) of distribution systems can be coordinated for all fault current values involving single feeders. However, it is vulnerable to Multiple Feeder Faults (MFF), which involve at least two feeders simultaneously, leading to the incoming feeder relay trip faster than the faulted feeder relays. In this case, all feeders connected to the power transformer are de-energized, even the healthy ones, directly impacting the network reliability, service quality and availability of the electricity utilities and ultimately leading to outage costs for the customers. In light of this, an IEC 61850-based OCPF scheme with the directional element is proposed to support existing OCPF to deal with MFF and encompass the integration of distributed generation, and can be directly implemented in the digital substations without requiring further equipment installation. Moreover, a hardware-in-the-loop platform is developed for testing the interoperability of the proposed scheme with multi-vendor protection relays, which can also assist electricity utilities in the validation of their protection and control schemes based on their requirements before the field implementation. Test cases are specifically elaborated to study the interoperability of the proposed scheme with three real devices—whose configuration details are also provided to aid protection engineers—in a real distribution system under different conditions such as switching operations, MFF types, resistance, location, and integration of distributed generation. The results show that the proposed scheme manages to enhance the selectivity and reliability of the digital substation protection system, hence representing a valuable complement to existing OCPF schemes.

INDEX TERMS Hardware-in-the-loop, IEC 61850, interoperability testing, multiple feeder faults, overcurrent protection function, real-time digital simulator.

NOMENCLATURE

CB	Circuit Breaker.
CID	Configured IED description.
DA	Data Attribute.
DG	Distributed Generation.
DO	Data Object.
GGIO	Generic process input-output.
GOOSE	Generic object-oriented substation events.
HIF	High Impedance Fault.
HiL	Hardware-in-the-Loop.
HV	High Voltage.
IED	Intelligent Electronic Device.
LD	Logical Device.
LN	Logical Node.
LV	Low Voltage.
MFF	Multiple Feeder Faults.

The associate editor coordinating the review of this manuscript and approving it for publication was Fanbiao Li.

MFFPF	MFF protection function.
OCPF	Overcurrent protection function.
PEA	Provincial Electricity Authority of Thailand.
RCA	Relay Characteristic Angle.
rINC	Incoming feeder relay.
rOC	Overcurrent relay.
rOUT	Outgoing feeder relay.
rTB	Overcurrent relay at the tie bus.
RTDS	Real-Time Digital Simulator.

I. INTRODUCTION

The service availability and continuity of the distribution systems are the key issues that many electricity utilities must take into account while providing customers with electricity. Customers require continuity in electricity supply, especially industrial customers, since every outage event interrupts their production process. The outage events caused by the faults in the distribution systems lead to an economic loss on the customer side, referred to as the ''outage cost'', which can amount even up to tens of thousands of EUR/event/customer in the case of large commercial and industrial customers [1], [2]. In light of this, an essential requirement for modern power systems and the corresponding protection techniques and schemes is the capability to deal with various kinds of fault events caused by several factors such as weather conditions, environment, equipment, operation and human interference. In this regard and with respect to the arc flash protection caused by equipment malfunctions, several overcurrent protection function (OCPF) schemes have been developed in commercial Intelligent Electronic Device (IED)s and implemented by using the generic object-oriented substation events (GOOSE) communication service. For example, [3] proposed the use of GOOSE to protect arc flash in the switchgear that consists of two bus bars, eight breakers, and cable compartments for high-speed tripping by employing light and current sensors. The results of this work indicated that the tripping time is fast enough to separate the arc fault from the system before the equipment is damaged. As another example of using GOOSE for protection schemes, the OCPF scheme proposed in [4] deployed GOOSE to exchange blocking signals among overcurrent relay (rOC)s at the upstream and downstream substations with definite time coordination in a radial system. Furthermore, [5] proposed a protection scheme to identify the fault location in the distribution system using GOOSE and sampled value (SV) for the directional element of the OCPF. However, this technique requires additional devices to route the GOOSE and SV for signal exchange. Moreover, to identify the fault location, this scheme requires sensors to be installed in each feeder. Consequently, with this technique, the number of required sensors may become prohibitively large for high-dimensional systems.

There are also studies that consider system reconfigurations while developing protection schemes for power systems. For instance, [6] and [7] propose OCPF schemes taking into consideration the adaptive settings using GOOSE to change the setting groups of the OCPF once the system configuration changes. However, to change the setting group of the OCPF, the IED requires to re-boot itself. As the re-boot period may take some time and if the fault occurs in the meanwhile, the IEDs are temporarily disabled, hence not being able to operate and clear the fault from the system.

In practice and mainly due to economic reasons and the limitations brought by the right of way, the structure of many distribution systems (especially in North and South America and South-East Asia) is designed and constructed to contain multi-feeder overhead lines on the same pole. In such cases, the nature of overhead lines makes them prone to external disturbances caused by thunderstorms, fallen trees, and trucks or cars crashing on them. In addition to the above-mentioned external disturbances, switching operations within distribution systems which aim at reducing congestion problems by transferring load among adjacent feeders can potentially lead to operational disturbances. This can happen if the switching action is accompanied by high arc currents. The above-mentioned external and operational disturbances are the main causes of Multiple Feeder Faults (MFF), i.e., faults involving more than one feeder simultaneously. As such faults are inevitable in distribution systems consisting mainly of overhead lines, it is important to investigate and consider them while designing protection schemes for such distribution systems.

The above-mentioned state-of-the-art OCPF of the relays at the substation can be coordinated for all fault current values involving single feeders. However, such protection schemes with proper coordination among primary and backup protection for all fault current values face difficulties when it comes to MFF occurrence in the system. Such faults lead to the miscoordination of the OCPF of the relays at the substation as they lead to the triggering of the OCPF of the incoming feeder relay (rINC) and its consequent faster tripping than the outgoing feeder relay (rOUT) [8]. As a matter of fact and for MFF, all feeders connected to the power transformer (including the healthy feeders) are de-energized. This directly affects the continuity, reliability, and quality of the service of the electricity utilities and makes the existing OCPF vulnerable to MFF. Moreover, the OCPF of [3], [4], [5], [6], and [7] are not able to address the MFF as they have been developed to deal with a single fault occurring in one specific feeder. Although [8] deals with MFF, the protection scheme proposed in this study has been implemented with the non-directional OCPF which might result in an unexpected operation in the case of distributed generation (DG) connection into the network which has not been addressed in this work. It is noteworthy that there are research studies that take into consideration the connection of DGs while developing protection schemes for distribution systems such as the one proposed in [9]. However and to the best of authors' knowledge, such schemes cannot deal with MFF and are only suitable in the case of single-feeder faults.

On the path towards the digitalization of automation systems, the hard-wired communication among different IEDs is being substituted by modern communication infrastructure. In fact, the modern protection and control systems depend heavily on the communication infrastructure and the capability of the system's components to appropriately interoperate and communicate among devices and systems [10], [11], [12], [13], [14]. For the seamless transition from conventional substations to digital ones, the IEC 61850 standard series play a crucial role by providing a set of guidelines with the ultimate goal of improving the availability and quality of the service for the customer. There have been some attempts in the literature to follow the above-mentioned IEC 61850 guidelines, which have led to either the partial conversion of conventional substations into digital ones at the bay and station levels or their full conversion with the addition of process level, too [15]. Consequently, the conventional testing and commissioning procedures, which were suitable for conventional protection and control schemes, shall also be substituted by modern testing approaches in order to validate the performance of the protection and control schemes developed specifically for modern digital substations and check their interoperability with multi-vendor IEDs. In this regard, some previous works have proposed different IEC 61850-based testing platforms to evaluate the performance of protection and control schemes. For example, [16], [17], and [18] propose IEC 61850-based testing platforms for co-simulation between software and hardware to evaluate and analyze the performance of the protection scheme and protection function using real-time simulation. In such studies though, the focus is not on testing the interoperability of the proposed schemes with IEDs from different vendors at the bay level. It is noteworthy that such interoperability testing for digital substations is of great importance as it ensures that IEDs from different vendors can appropriately interoperate and communicate with each other before being implemented in the field.

In view of the gaps in the above-mentioned literature, this paper provides the following contributions:

- An IEC 61850-based protection scheme—henceforth referred to as MFF protection function (MFFPF)—is proposed to address MFF and encompass the integration of DG in distribution systems. The proposed MFFPF is elaborated with the directional element, uses GOOSE for the message exchange and can effectively support and complement existing OCPF to make them capable of dealing with MFF. Furthermore, the proposed MFFPF can be implemented in the digital substations of electricity utilities with the internal logic and programming of the IEDs without the need for additional equipment installation. Moreover, if the configuration of the system changes, with the proposed scheme there is no need for the IED to reboot itself.
- A Hardware-in-the-Loop (HiL) platform is developed to test the interoperability of the MFFPF with multi-vendor IEDs at the bay level of the digital substation. The interoperability testing is accomplished by measuring the performance of the MFFPF in terms of the tripping time—i.e., the elapsed time between fault inception and the reception by the Real-Time Digital Simulator (RTDS®) of the signal coming from IEDs—under different conditions (such as location, type and resistance of the MFF) and for different scenarios (e.g., considering various switching operations and the connection of DG). The developed testing platform can be easily adapted to assess other protection schemes (e.g., breaker failure protection functions).
- An explanation of how to configure three commercial IEDs and the GSE module of RSCAD® is presented to accomplish the information exchange based on Configured IED description (CID) files to perform the proposed scheme. In particular, the IEDs under test—provided by vendors from SEL (SEL 751), Schneider (Schneider P543), and ABB (ABB REF615)—are specifically chosen as they implement different protection approaches for fault detection. Therefore, utilities can replicate this concept with other protection and control schemes.

This paper is organized as follows. Section II describes the characteristics of MFF. In Section III, the proposed IEC 61850-based scheme is introduced; Section IV describes the testing platform developed for interoperability testing; Section V provides the details of the configuration of the three commercial IEDs under test. Section VI presents the case study adopted in this work to describe the proposed scheme and verify its interoperability with the IEDs under study. Section VII presents the simulation results of three selected test cases; Section VIII concludes the paper. Section IX discusses issues on interoperability testing and paves the way for future work.

II. MULTIPLE FEEDER FAULTS IN DISTRIBUTION SYSTEMS

As mentioned in Section I, MFF can originate from natural or artificial events (e.g., thunderstorms, fallen trees, switching operations, and accidents) occurring in multi-feeder overhead lines, like in Fig. 1.

To describe the MFF and its effect on the coordination of the existing OCPF, consider Fig. 2, where the configuration of a substation with 2 buses and 10 feeders is depicted. During the normal operation, the tie bus circuit breaker (CB) is open, whereas the "Incoming 1" CB, "Incoming 2" CB, and all the Outgoing CBs are closed. For many utilities, the coordination of the rOC at the substation is calculated and designed based on the inverse time characteristic:

$$t = \frac{TMS \times A}{\left(\frac{I}{I_s}\right)^{\alpha} - 1} \tag{1}$$

where TMS is the time multiplier setting, I and I_s are the values of measured current and relay setting current, respectively. For the normal inverse time characteristic, A and α are represented respectively by 0.14 and 0.02, whereas

FIGURE 1. The multi-feeder structure of the distribution lines (author's personal picture).

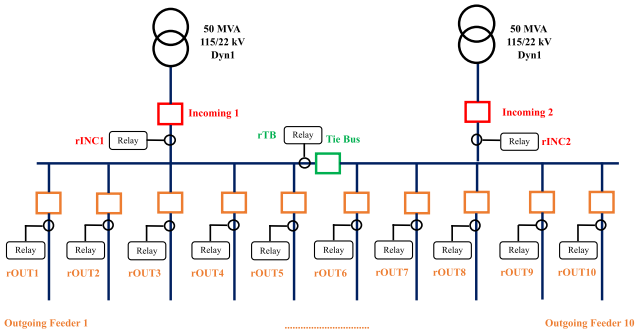

FIGURE 2. General substation configuration.

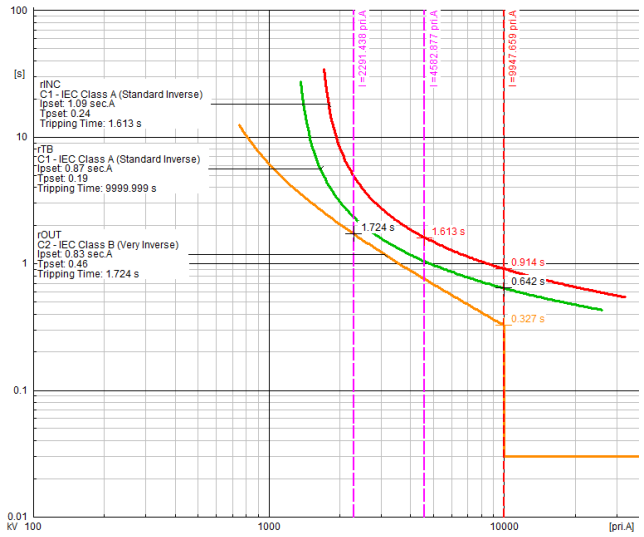

FIGURE 3. Overcurrent coordination of the relays at the substation.

for the very inverse characteristic, A and α are represented respectively by 13.5 and 1. In addition, the coordination is calculated using the maximum fault current magnitude of both phase and ground faults at the Low Voltage (LV) bus, and the margin between primary and backup rOCs is between 0.3 and 0.4 s [19]. The coordination of the rOCs on the 22kV side and based on the substation configuration shown in Fig. 2 is shown in Fig. 3. In Fig. 3, a maximum three-phase fault at the LV bus is represented by a dashed red line. For a single feeder fault, rOCs at the substation are able to coordinate to distinguish a feeder fault for all fault current values with the minimum margin at 0.3 s. Two simultaneous feeder faults are used as an example to describe the characteristics of MFF. In this case, the purple-dashed lines of Fig. 3 represent the MFF occurring in the system between "Outgoing Feeder 1" and "Outgoing Feeder 2". Once the MFF occur in the system, the fault magnitude seen by the rINC is approximately two times greater than that seen by the rOUTs: this results in the rINC tripping faster than rOUTs (1.613 s vs 1.724 s). In this case, all feeders (even the healthy ones) connected to the power transformer are de-energized leading to the outage event in wide areas. More in detail, Fig. 4 represents the disturbance record of the MFF. The operation of the rOC based on the inverse time characteristic can be calculated using (1); hence the operating times of the rINC and rOUTs to respond with the MFF of two feeders are:

$$t_{rINC} = \frac{0.24 \times 0.14}{\left(\frac{6,687}{1,635\times\sqrt{2}}\right)^{0.02} - 1} = 1.565\ s \tag{2}$$

$$t_{rOUT1} = \frac{0.46 \times 13.50}{\frac{3,291}{498\times\sqrt{2}} - 1} = 1.691\ s \tag{3}$$

$$t_{rOUT2} = \frac{0.24 \times 13.50}{\frac{3,250}{498\times\sqrt{2}} - 1} = 1.718\ s \tag{4}$$

The operation of the rOC shown in Fig. 4 has been calculated based on the RMS value [20], [21], [22]. Moreover, setting the trigger of the relay for showing the pickup or starting signals to trigger the event creates lots of undesired events in the disturbance record during routine situations, i.e., overcurrent due to on-load switching among feeders or within the feeder, motor starting, etc. Setting the trigger leads to utilizing too many memory resources of the IED. Therefore, if the rINC operates, there is no indication showing at the faulted feeders' relays (rOUTs). In this sense, the operators at the control center do not know which feeders are the faulted feeders, and it takes a long time to find the latter and restore the system, impacting the continuity of energy supply to the customers which are connected to healthy feeders.

In case one of the power transformers needs to be maintained, another power transformer must supply energy to all the feeders (10 feeders for 2 buses and 15 feeders for 3 buses). In this case, the tie CB must be closed, and one of the incoming CBs needs to be opened. The MFF lead to the overcurrent relay at the tie bus (rTB) trip faster than the faulted feeders' relays (rOUTs); this results in a wide-area outage event, which is the same situation happening to rINC and rOUT. Hence, it can be noticed that the existing OCPF is vulnerable and cannot deal with the MFF.

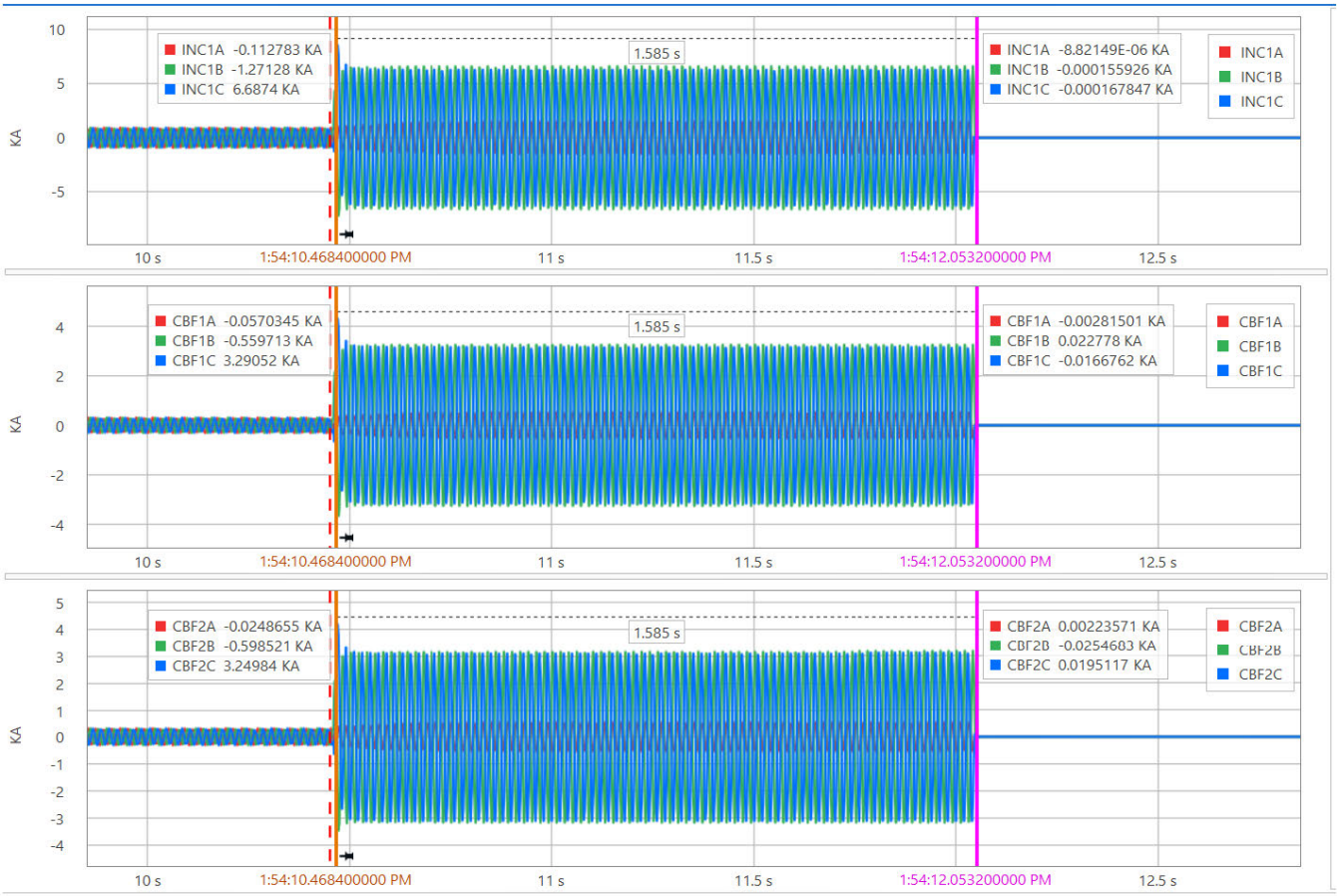

FIGURE 4. The current waveforms of the rINC (INC1), rOUT1 (CBF1) and rOUT2 (CBF2) relays once the multiple feeder fault occurs in the distribution system.

III. PROPOSED SCHEME FOR MULTIPLE FEEDER FAULT PROTECTION

To deal with the MFF in the distribution system and prevent the wide-area blackout caused by the rINC operating faster than the faulted feeder relays rOUTs, an MFFPF is developed based on the GOOSE communication protocol defined in the IEC 61850 standard. By developing a protection scheme based on IEC 61850, interoperability can be attained to perform the information exchange among devices, or between devices and systems [23], as no proprietary protocol is needed and no vendor-specific device is required. In this way, the proposed MFFPF can be implemented in the digital substations of electrical utilities with the internal logic and programming in the IEDs without requiring any additional equipment installation.

The logical architecture of the MFFPF is shown in Fig. 5. The operation of the proposed scheme and the information flow between rOCs, rINC, and rTB are detailed hereafter.

A. OUTGOING FEEDER RELAYS

Once the MFF occur in the system, rOUTs detect them by themselves and have to wait for the signals from other rOUTs to confirm that the MFF have occurred in the system. Then, rOUTs release the trip signals to open the CBs of the faulted feeders. A delay time of 100 ms is used for the MFFPF to avoid nuisance operation caused by a transient event in the system, e.g., on-load switching in a feeder, motor starting, etc. Each rOUT needs to be configured for publishing both phase and ground directional elements to the other relays in order to proceed according to the MFFPF. For the subscribing part, rOUT receives the signal from other rOUTs, from the rTB (e.g., once rTB is to be closed for specific purposes such as maintenance), and from the rINC (e.g., once the operator needs to disable the MFFPF in the case of the maintenance).

Once a DG is connected to the system, unexpected operation of the MFFPF may occur due to the DG in-feed effect: for instance, in the case a fault occurs on the adjacent feeder, the rOUT detects the fault in the reverse direction. Hence, to enhance its selectivity in the presence of DG, the MFFPF is implemented with the directional element.

B. TIE BREAKER RELAYS

rTB provides both phase and ground non-directional elements for the rOUTs, as the current can flow in two directions. The GOOSE signal from the rTB is sent once the tie CB is closed to connect buses at the substation. The rTB does not have

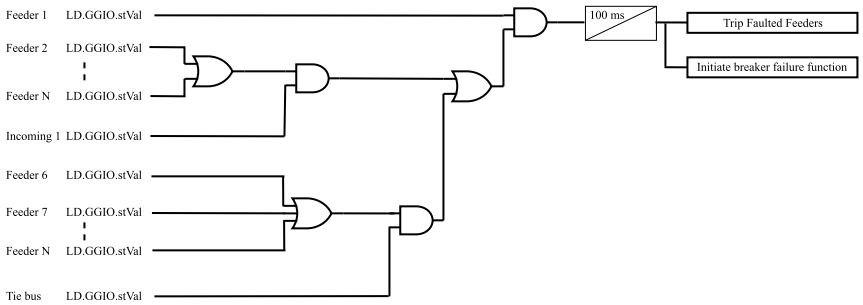

FIGURE 5. Logical architecture of the proposed protection scheme for multiple feeder fault protection.

to subscribe to the GOOSE signal, as the rOUTs receive the GOOSE signal from the rTB and decide to clear the MFF from the system. The tie CB is closed once one of the power transformers at the substation cannot be energized or need to undergo maintenance.

C. INCOMING FEEDER RELAYS

rINCs are used to provide the GOOSE signal for disabling the MFFPF during the maintenance period. By design, the rINC receives the status "ON" and "OFF" from the cut-off switch installed at the switchgear panel, which can be controlled remotely by the control center as well as locally at the substation.

D. IEC 61850 DATA MODEL OF THE PROPOSED SCHEME

The IEC 61850-based MFFPF is implemented with the data model illustrated in Fig. 6, which is constituted by:

- the Logical Device (LD), which represents the name of the physical IED;
- the "Generic process Input/Output (GGIO)" Logical Node (LN), which is used to represent the MFFPF;
- the "Ind" Data Object (DO), which represents the information exchanged (in the form of binary output), belonging to the single point status (SPS) common data class;
- the "stVal" Data Attribute (DA), which contains a boolean signal for the MFFPF.

With such a hierarchical data model, the information between devices from different vendors can be exchanged based on the Substation Configuration Language (SCL) [24], [25]. In particular, the data model shown in Fig. 6 is used to represent the MFFPF, as no LN is associated with the MFF protection function generally provided inside IEDs. Moreover, this data model is used to contain the GOOSE signal for all relays at the substation because the GOOSE signals of the rOUT and rTB—coming from the tie CB status, phase and ground fault detection—can be grouped and published as a single boolean signal. As some manufacturers pose a limitation on the number of the GOOSE input signals, these are grouped into one single boolean signal. This reduces the number of GOOSE inputs to the GOOSE subscriber and

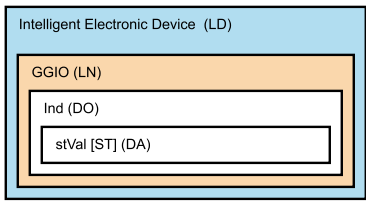

FIGURE 6. Logical node used for the proposed scheme.

TABLE 1. Status of the MFFPF signal.

Logical expression	Binary value
LD.GGIO.IndX.stVal [ST] = "ON"	1
LD.GGIO.IndX.stVal [ST] = "OFF"	0

ultimately facilitates the protection engineers in conveniently testing the MFFPF.

The full path of the hierarchical data model that represents the status "ON" and "OFF" of the MFFPF is shown in Table 1, where [ST] refers to the functional constraint "status information" of the "stVal" DA.

E. OPERATION OF THE OVERCURRENT PROTECTION FUNCTION

In the proposed MFFPF, two approaches for fault detection are implemented, namely the positive/negative sequence and Relay Characteristic Angle (RCA) operation modes, which are described hereafter.

1) POSITIVE/NEGATIVE SEQUENCE OPERATION MODE

The positive/negative sequence operation mode is represented by:

$$(-90^\circ + \Theta_{Z_1}) < \widehat{\Theta}_{Z_1} < (90^\circ + \Theta_{Z_1}) \tag{5}$$

$$Z_2 = \frac{1}{I_2^2} Re[\overline{V_2}(\overline{I_2} \times 1\angle\Theta_{Z_1})^\star] \tag{6}$$

$$threshold = \begin{cases} Z_{2F} > 0, & 1.25 \times Z_{2F} - 0.25 \times |\dfrac{V_2}{I_2}| \\ Z_{2F} \leq 0, & 0.75 \times Z_{2F} - 0.25 \times |\dfrac{V_2}{I_2}| \end{cases} \tag{7}$$

TABLE 2. Measured voltage and current for phase fault detection.

Phase	Current	Voltage
A	I_A	V_{BC}
B	I_B	V_{CA}
C	I_C	V_{AB}

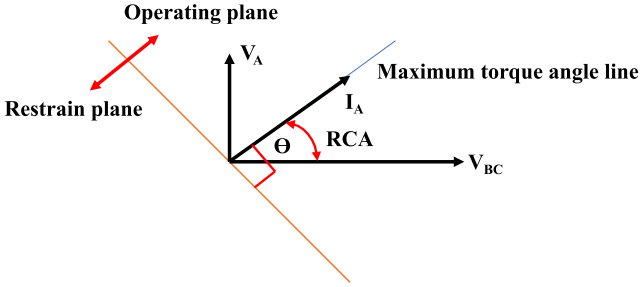

FIGURE 7. Phase fault detection based on 90° connections.

where:

- $\overline{V_2}$ and V_2 are the complex value of the negative sequence voltage and its magnitude, respectively;
- $\overline{I_2}$ and I_2 are the complex value of the negative sequence current and its magnitude;
- Θ_{Z_1} is the positive sequence impedance angle;
- $\widehat{\Theta}_{Z_1}$ is the operating plane;
- Z_{2F} is the forward/reverse fault threshold.

It is noteworthy that Eq. (5) is used to enable the directional 32PF element, which is the relay word bit of SEL relay for three-phase fault detection. This element measures the positive sequence to calculate the operating plane.

Eqs. (6) and (7) are used to enable the directional 32QF element for phase-to-phase, phase-to-phase-to-ground, and single-phase-to-ground faults detection since these three fault types generate negative-sequence current and voltage. Regarding the 32QF element, Z_2 is compared with the forward fault threshold Z_{2F}; if Z_2 is less than Z_{2F}, the 32QF element declares a forward fault. On the other hand, if the Z_2 is larger than Z_{2F}, the 32QF element declares a reverse fault [20], [26]. The operation of the 32PF and 32QF directional elements distinguishes the fault based on the R-X plane.

2) RELAY CHARACTERISTIC ANGLE OPERATION MODE

In the RCA operation mode for fault detection, the phase-to-phase voltage and the opposite phase current are measured to detect phase fault, as shown in Table 2, generally according to 90° connections (operating plane, ± 90° from maximum torque line), as shown in Fig. 7.

The RCA for phase fault detection depends on the system characteristic. For example, (i) 30° is recommended for the system with a low R/X ratio and plain feeders with zero sequence source behind the relay, (ii) 45° is recommended for the transformer feeders with zero sequence source in front of the relay, and (iii) 60° is recommended for the system with a small section of cables [19]. In this work, RCA is chosen to be equal to 30°.

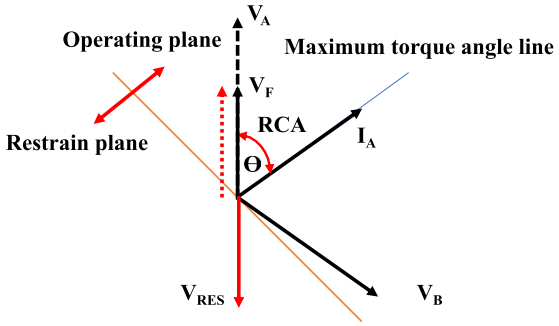

FIGURE 8. Ground fault detection based on 90° connections.

For ground fault, the residual voltage ($-3V_0$) is used to detect phase-phase-to-ground and phase-to-ground faults, as shown in Fig. 8. The relay characteristic depends on the system grounding [19]. For instance, (i) 0° is recommended for the resistance-earthed system, (ii) –45° for the distribution system with solidly-earthed, and (iii) –60° for the transmission system with solidly-earthed.

IV. TESTING PLATFORM ARCHITECTURE

To verify the interoperability of the proposed MFFPF with physical (potentially multi-vendor) IEDs, the testing architecture of Fig. 9 is developed, which consists of HiL connection of RTDS®, power amplifiers, and the devices under test.

All binary signals (such as starting signal, tripping signal, CB status, as well as enable/disable signals) are exchanged using GOOSE messages and represented in Fig. 9 by red lines, whereas voltage and current signals are represented by the orange and blue lines, respectively.

A. REAL TIME DIGITAL SIMULATOR

RSCAD is used to model the power system, and the simulation of faults and the exchange of the binary signals (i.e., CBs status, protection and control signals as well as the transmission of the voltage and current analog signals to the actual devices connected to the testing platform) are carried out by the NovaCore processing unit of RTDS®. The analog signals are sent to the power amplifiers interfaced with the testing platform via the GTAO module (available in the RSCAD software), which directly interfaces with the physical GTAO card of RTDS®. The analog signals from the power system model are transmitted to the power amplifiers within ranges of ±10 V. In this case, the analog signals are sent to the amplifiers via a wired connection from the GTAO card, and the NovaCore processor is connected to the GTAO via the fiber optic cable (GT port). The scaling factor for each analog channel of the GTAO module needs to be defined according to the gain of the amplifier and the required values of the analog signals for IEDs. For the exchange of the boolean signals among RTDS® and physical devices under test, the GTNETx2 card is required. The GTNETx2 card is connected

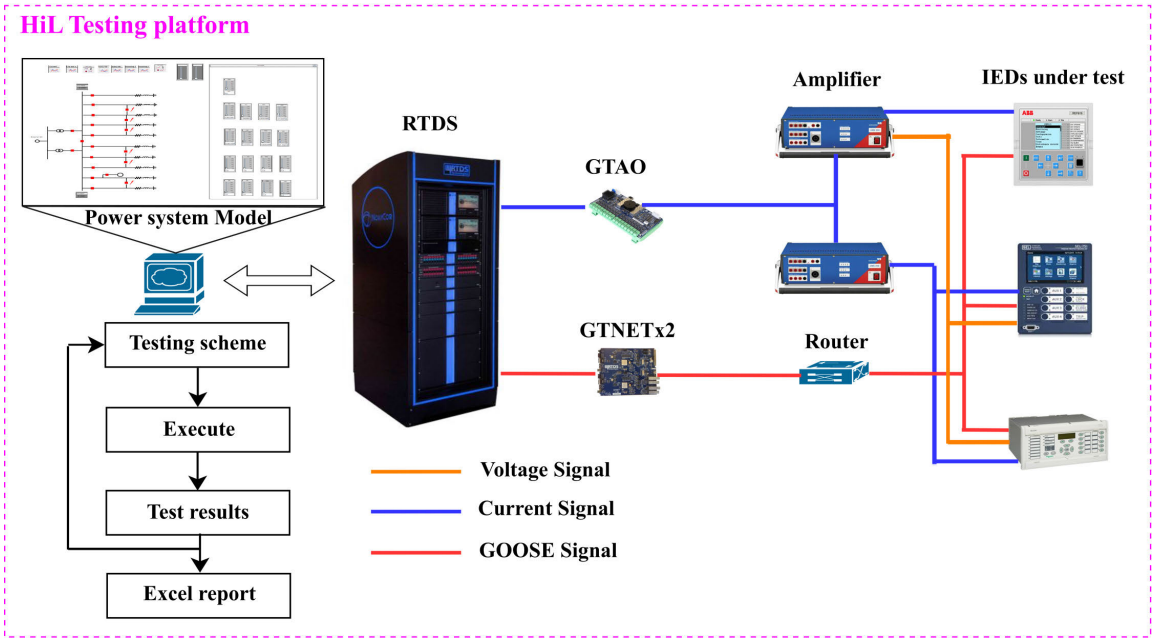

FIGURE 9. The proposed HiL platform for the interoperability testing in this work.

to the NovaCore processor with the fiber optic cable via GT port and to the testing platform with the RJ45 cable. Several protocols can be installed within the GTNETx2 card, but only four can be selected, and only one protocol at a time can be activated. For the developed testing platform, GOOSE protocol is activated. The GOOSE signals can be sent out from RTDS® to the physical equipment via the GTNETx2 card using the GSE module, which directly interfaces with the GTNETx2 card, for preparing the configured information (CBs status, disable/enable signals of the proposed scheme) to be published to the local area network (LAN) via a router. In order to receive the GOOSE signals from the IEDs, the word-to-bit converter element is required to map the GOOSE signals from the IEDs by converting the multiple-word integers into multiple logical signals. The interoperability testing is automatically carried out by means of an ad-hoc developed script file in C-type programming language. Therefore, the configuration of the testing environment and testing scenarios, including the required parameter changes, can be done automatically.

B. INTELLIGENT ELECTRONIC DEVICES UNDER TEST

Three IEDs from different vendors are considered as devices under test and integrated into the testing platform. The IEDs receive the voltage and current signals from the secondary side of the voltage and current transformers. In this work, ideal transformers of the CT and VT are deployed. The saturation of the instrument transformers is not taken into account. The CT ratio of the rINC and rTB is 1500A:1A, and 600A:1A for all rOUTs; the VT ratio is 22kV:110V. Additionally, rOUTs require the three-phase voltage signal to be polarized for the directional element to declare the forward and reverse directions of the fault in the system. The starting and tripping signals are sent back to the RSCAD for evaluation and validation.

C. AMPLIFIERS

Two power amplifiers— which can be configured via a web interface—are used to amplify the voltage and current magnitude for the IEDs from the GTAO and accurately generate analog voltage and current signals on the secondary side. In the developed testing platform, the analog input range of ± 7.071 Vpeak (5 Vrms) is adopted. One amplifier is configured to generate both current and voltage signals (3×300V and 3×32A), and the other one is configured to generate only current signals (6×32A) for the IEDs. The amplification of these two amplifiers at a 5 Vrms input range is 60V:1V for the voltage signals and 6.4A:1V for the current signals [27]. These amplifiers are connected to the GTAO card and IEDs via a wired connection.

V. CONFIGURATION OF THE DEVICES UNDER TEST

Considering the MFFPF, to implement the directional element from different vendors, the CID file needs to be created for exchanging information among relays at the substation based on the MFFPF. In this regard, to verify that the IEDs can interoperate with the MFFPF, the testing platform of Section IV is used. The CID file of each relay and RTDS® is configured using the proprietary software from the manufacturer. In particular, the SEL751 relay requires the AcSELerator Quickset software to configure the overcurrent protection element, and the AcSELerator Architect software is used to configure the GOOSE signal. The Schneider P543 relay requires the Easergy Studio software to configure both

the overcurrent protection element and the GOOSE signal. The ABB REF615 relay requires the PCM600 software to configure both the overcurrent protection element and the GOOSE signal. In this work, the signal used to enable and disable the MFFPF is provided by RTDS®, assumed to be the control center. Each relay also receives the circuit breaker status from RTDS® via the GOOSE signal. The steps to publish and subscribe to GOOSE messages between relays and RTDS® are reported hereafter.

A. GOOSE PUBLISHING

1) SEL 751

To configure GOOSE publishing and the starting signal of phase and ground directional element, the AcSELerator Architect and Quickset are needed. First, SELogic Variable (SV) is determined for containing the relay word bits, namely 67P2P and 67N2P in the Quickset. The starting values for 67P2P and 67N2P have to be defined for the current detection of the 50P2 parameter (level 2). Then, the SEL-751 data model is created in Architect for generating the dataset and the GOOSE transmission. During this step, the dataset under GGIO needs to be defined with the information configured in the SV. For example, the starting signal for phase and ground directional element is defined as ANN.SVGGIO3.Ind09.stVal (the GOOSE output signal has been assigned to the GGIO3). Then, the defined dataset needs to be enabled on the GOOSE transmit tab for publishing the GOOSE message.

2) SCHNEIDER P543

Easergy Studio software is used to configure the relay setting, logical process (PSL module), and dataset definition (MCL 61850 module). For the starting phase and ground directional elements, level 1 of the current detection is used to publish the GOOSE signal using virtual output, which is available in the PSL module. Then, the dataset is created using the MCL module based on the information configured in the PSL module. Since the GOOSE output signal in the PSL module has been assigned to the GosGGIO2, the data object (IndX) and data attribute (StVal) of the virtual output (GOOSE output signal) are assigned to the GosGGIO2 LN. In the last step, for publishing GOOSE into the LAN network, the configured dataset needs to be selected as a reference in the GOOSE publishing tab.

3) ABB REF615

The PCM600 is needed to configure the parameter settings of the OCPF and create the dataset using IEC 61850 configuration module. The non-directional overcurrent element is used for publishing the GOOSE message, and level 1 of phase and ground fault detection contained within the DPHLPTOC1 and EFHPTOC1 logical nodes are implemented under XGGIO110. In this sense, the XGGIO110 needs to be created in the Application configuration module by combining both phase and ground detection. After creating the XGGIO110, in the IEC61850 configuration module, XGGIO110 is contained within the LD named LD0, then the data hierarchy named LDO.XGGIO110.Ind0X.stVal can be configured for integration into the dataset.

4) RTDS

For the proposed testing platform, RTDS® needs to be configured to publish the signal to enable and disable the MFFPF as well as the CB status. The GTNET-GSE module, which is available in RSCAD is used to provide the information for publishing. First, the ICT IEC61850 project needs to be created using the GTNET template to represent the GTNET component and IED in the project. Then, the GOOSE output signals implemented with GGIO LN must be created and mapped with the disable/enable signal and circuit breaker status provided in the power system model. After the dataset definition step, the publishing part needs to be defined by determining the LD name and selecting the information provided in the dataset to be contained in the assigned LD. For example, protection.OUT_GGIO1.Ind01.stVal is used to publish the enable/disable signal to the IEDs.

Regarding the dataset of each IED, the following four parameters have to be defined:

- Multicast MAC address: this parameter has to be uniquely defined, as it is used to identify the IED that will publish the GOOSE signal into the LAN network; the MAC address suggested in the IEC61850 standard should range from "01-0C-CD-01-00-00" to "01-0C-CD-01-01-FF" [28].
- APP ID: this parameter relates to the GOOSE message and is also used to verify the message, which is sent by the sender to the correct receiver [16].
- VLAN ID: this parameter is employed to identify the IED, which publishes a GOOSE message to the LAN network. Furthermore, it is also used to filter the system's traffic [16].
- VLAN Priority: this parameter is used to prioritize the GOOSE message to prevent delays caused by other messages in the communication network [29]. This parameter can range from 0 to 7; in the case it is not configured, its default value is 4.

B. GOOSE SUBSCRIBING

Since the information contained in the dataset is used to create the CID file for exchanging information between IEDs based on the XML schema, the CID file from each IED needs to be exported and imported using proprietary software from the IED manufacturers. Hence, the steps required to subscribe to the GOOSE message from other vendors' IEDs are given hereafter.

1) SEL751

To subscribe to the GOOSE signals, the CID files from other IEDs need to be imported into the Architect (IED palette). In the next step, the CID file of the IED is imported into the

project file and the signals associated with the virtual bit (VB) configured in the Quickset are mapped. In this case, VB001 is reserved for the disable/enable signal, VB002 for the circuit breaker status, and VB003 for MFFPF.

2) SCHNEIDER P543

To map the GOOSE signals using MCL61850, the CID files from other vendors' IEDs need to be employed as a dataset reference for each GOOSE signal. The signal needs to be mapped to the virtual input (GOOSE input signal) that is configured in the PSL module. In this case, virtual input 1 is mapped with the disable/enable signal, virtual input 2 for the circuit breaker status, and virtual input 3 for the MFFPF.

3) ABB REF615

As the ABB relay is used to represent the rINC and rTB, the relays at these two locations do not require subscribing to the GOOSE signal from other relays.

4) RTDS

The CID files from IEDs need to be imported into the ICT project, and the GOOSE input signal is mapped with IN_GGIO LN. In this case, ten GOOSE input signals from IEDs from three vendors are mapped. Schneider P543 and SEL751 provide starting and tripping signals originated by the directional OCPF, including the tripping signal generated by the MFFPF to the RTDS®; the remaining signals (starting and tripping signals of phase and ground OCPF) are provided by ABB REF 615.

VI. USE CASE UNDER STUDY

To verify the interoperability of the MFFPF with the IEDs under test, a use case has been specifically developed. In particular, a portion of a real distribution system of the Provincial Electricity Authority of Thailand (PEA), which is depicted in Fig. 10, is modelled in RTDS®. The parameters of the power system model, which consists of two buses and five feeders each, are shown in Table 3. The distribution line length (25 km) reflects the average length in areas covered by large commercial and industrial customers. RTDS® is employed to exchange the real-time signals among the physical devices, whereas Digsilent Power Factory software is adopted to obtain the equivalent parameters from the power plant to the interested/selected substation for this study.

The devices under test are three real IEDs, namely ABB REF615, SEL 751 and Schneider P543. In particular, ABB REF615 is used to represent the relay at the LV side of the power transformer and at the tie CB (rINC1 and rTB), whereas, as feeder relays, Schneider P543 is used to protect feeder 1 (rOUT1) and SEL 751 is used to protect feeder 2 (rOUT2). The overcurrent settings for each relay, which are summarized in Table 4, are designed and coordinated based on the PEA's criteria [30]. A script is developed in RSCAD to carry out the test and the results of each test case are automatically recorded and saved in an excel file.

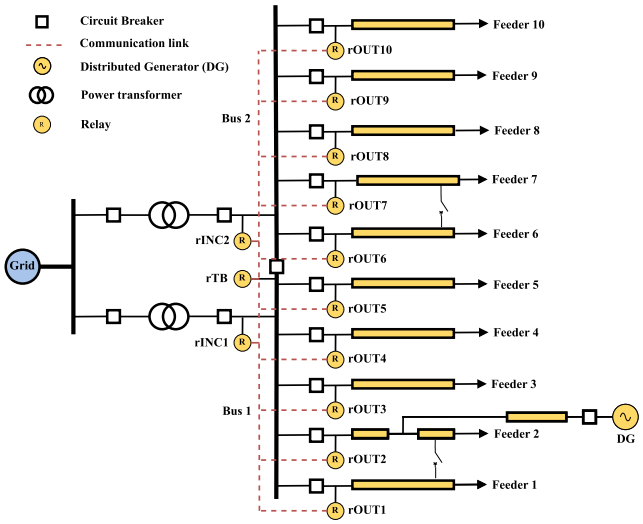

FIGURE 10. Power system model adopted for the use case under study.

TABLE 3. Parameters of the power system model.

Source parameters		
Positive sequence impedance	Z = 2.76 Ω	85.08°
Zero sequence impedance	Z = 3.47 Ω	86.26°
Power transformer at the substation		
Rated MVA		50 MVA
Rated Voltage (High Voltage (HV))		115 kV
Rated Voltage (LV)		23.10 kV
Short circuit impedance		13.80%
Vector group		Dyn1
Line parameters		
Positive sequence impedance	Z = 0.21 + j0.41 Ω/km	
Zero sequence impedance	Z = 0.35 + j1.63 Ω/km	
Power transformer at the point of common coupling		
Rated MVA		12.50 MVA
Rated Voltage (HV)		23.10 kV
Rated Voltage (LV)		6.60 kV
Short circuit impedance		10.00%
Vector group		YNyn0
Generator parameters		
Rated MVA		12.37 MVA
Rated Voltage		6.60 kV
Power factor		0.80
Direct Axis Synchronous Reactance, Xd		233.10%
Direct Axis Transient Reactance, X'd		21.60%
Direct Axis Sub-transient Reactance, X"d		15.60%
Negative Sequence Reactance, X2		17.10%
Zero Sequence Reactance, X0		7.30%

Three test cases are elaborated to specifically reflect scenarios of interest, including the effect of all possible switching operations as well as the potential connection of DG. In each test case, ten signals from three IEDs are sent back to the RSCAD once the IEDs detect the MFF emulated in the RSCAD. Moreover, each IED receives the CB status from the simulated power system via the GOOSE protocol for the breaker failure function. To enable the MFFPF, the Cut-off switch needs to be switched "ON" for all test cases.

The interoperability of the IEDs under test with the proposed MFFPF is evaluated by measuring the performance of the operation of the proposed scheme, and the interoperability

TABLE 4. Setting parameters of the three IEDs under test.

Information of the relay setting			
	rINC	rTB	rOUT
Manufacturer	ABB	ABB	SEL, Schneider
Model	REF615	REF615	751, P543
CT ratio HV	1500	1500	600
CT ratio LV	1	1	1
Phase overcurrent setting (50/51)			
Curve	SI	SI	VI
I>	1.09	0.87	0.83
TMS	0.24	0.19	0.46
I> >	-	-	16.60
Time (s)	-	-	Instantaneous
Ground overcurrent settings (50N/51N)			
Curve	SI	SI	VI
IN>	0.26	0.22	0.25
TMS	0.53	0.40	0.84
IN> >	-	-	16.60
Time (s)	-	-	Instantaneous

verdict is "pass" or "fail" according to:

$$\text{verdict} = \begin{cases} \text{"pass" if operating time} > 0 \\ \text{"fail" if operating time} = 0 \end{cases} \quad (8)$$

In practical terms, the interoperability testing is carried out by calculating the operating time, i.e., the time elapsed from the fault inception to the reception by the RTDS® of the binary signals coming from the IEDs. In case the operating time is null, the interoperability test verdict is "fail", signalizing that the proposed scheme cannot detect the MFF. However, in this case other protection functions will be activated to clear the MFF, such as High Impedence Fault (HIF) and/or existing OCPF functions already residing in commercial IEDs.

Such an interoperability testing is of paramount importance in that it can verify the effectiveness of the information exchange among IEDs based on the protection scheme before their field implementation. Moreover, conducting an interoperability testing before the field development allows identifying the interoperability boundary, i.e., the set of conditions (e.g., the values of MFF resistance, the type of MFF, the MFF location, etc.) that divides the interoperability region (i.e., where a "pass" interoperability verdict is recorded) from the non-interoperability region (i.e., where a "fail" interoperability verdict is recorded). This might ultimately lead to recommendations towards stakeholders such as electricity utilities, and directions for future investigations to comply with specific requirements.

VII. SIMULATION RESULTS

In this section, the power system model parameters of Table 3 as well as the parameter settings of the IEDs of Table 4 are deployed to elaborate three test cases by using the HiL testing platform of Fig. 9. In particular, the interoperability testing is carried out in three different test cases specifically designed to investigate the effect of all possible switching operations at the substation as well as the effect of DG connection on the proposed MFFPF. Ten MFF types are applied for all the test cases, which consist of single-phase-to-ground fault types (AG, BG, CG), phase-to-phase fault types (AB, BC, CA), and multi-phase-to-ground fault types (ABG, BCG, CAG, and ABCG). To validate the interoperability among IEDs, ten binary signals are sent from the IEDs to the RTDS® and the following names are used:

TABLE 5. Parameter values for the interoperability testing.

Fault Resistance (Ω)
0.001, 2, 4, 6, 8, 10
Fault distance (km)
5, 10, 15, 20, 25
Fault type
AG, BG, CG, AB, BC, CA, ABG, BCG, CAG, ABCG

- "SELStr" represents the starting signal, both phase and ground fault detection of the rOUT2.
- "SELTr" represents the trip signal, both phase and ground fault of the rOUT2.
- "P543Str" represents the starting signal, both phase and ground fault detection of the rOUT1.
- "P543Tr" represents the trip signal, both phase and ground fault of the rOUT1.
- "SELMF" represents the trip signal operated by MFFPF of the rOUT2.
- "P543MF" represents the trip signal operated by MFFPF of the rOUT1.
- "ABBEFStr" represents the starting signal of a ground fault detection of the rINC and rTB.
- "ABBEFTr" represents the tripping signal of a ground fault detection of the rINC and rTB.
- "ABBPHStr" represents the starting signal of a phase fault detection of the rINC and rTB.
- "ABBPHSTr" represents the tripping signal of a phase fault detection of the rINC and rTB.

In addition, "Cutoff" is the name used to indicate the cutoff status.

For each test case, 300 scenarios are performed by simulating MFF between feeder 1 and feeder 2 with the parameter values of Table 5. In particular, ten MFF types are applied for each location, with the fault resistance R_f varying from 0.001 to 10 Ω (reflecting typical to uncommon values of fault resistances in distribution systems) with steps of 2 Ω, and the location along the length of the line is varied from 5 to 25 km, with 5 km for each step.

A. TEST CASE 1: NO DG CONNECTED

The network topology of this test case is the power system model of Fig. 10 with no DG connected, both incoming CBs closed, and the tie CB open. This is a normal operation in which the power transformers at the substation can energize the two buses.

As shown in Fig. 11, the simulations performed with the parameter values of Table 5 reveal that lack of interoperability (according to Eq. (8)) is recorded only for the single-phase-to-ground fault types AG, BG and CG (red dots), with the others

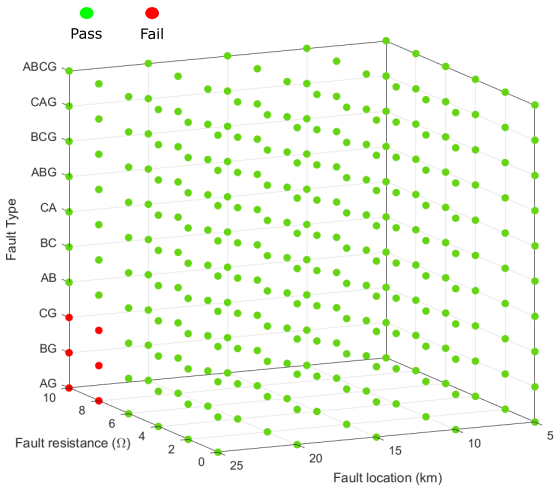

FIGURE 11. Test case 1. Interoperability verdict for rOUT1 of all fault types for different fault resistance values and fault locations. Same results are observed for rOUT2.

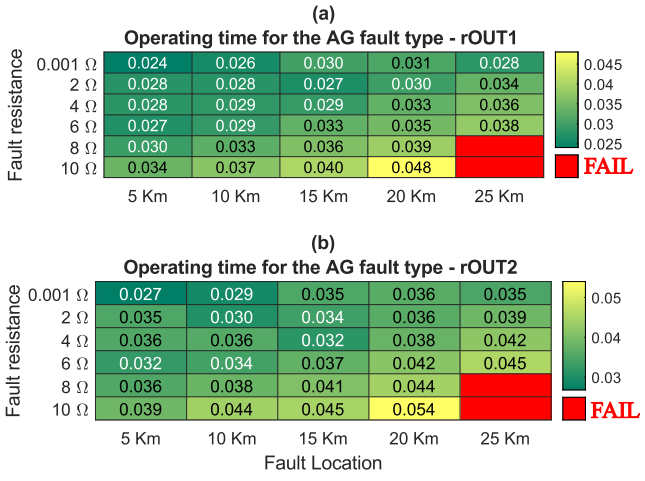

FIGURE 12. Test case 1. Operating times of rOUT1 and rOUT2 in the case of an AG MFF type for different fault resistance values and fault locations.

always leading to a "pass" interoperability verdict (green dots) for any location and any MFF resistance value.

More details can be observed in Fig. 12, which shows the operating times of the MFFPF for the two IEDs in the case of an MFF AG type. As it can be seen, the non-interoperability region (the red cells) is restricted to the area of $R_f \geq 8$ Ω and fault location at 25 km: for high values of MFF resistance, the rINC trips faster than rOUTs, resulting in a wide-area blackout. This behaviour is recorded also for BG and CG fault types. However, it is noteworthy that, due to the characteristics of MFF, at least two conductors of two feeders are involved, hence the single-phase-to-ground MFF are less likely to happen than the multi-phase-to-ground and phase-to-phase MFF. Nonetheless, if a single-phase-to-ground MFF happens with such a large R_f, the HIF function residing in commercial IEDs can deal with it.

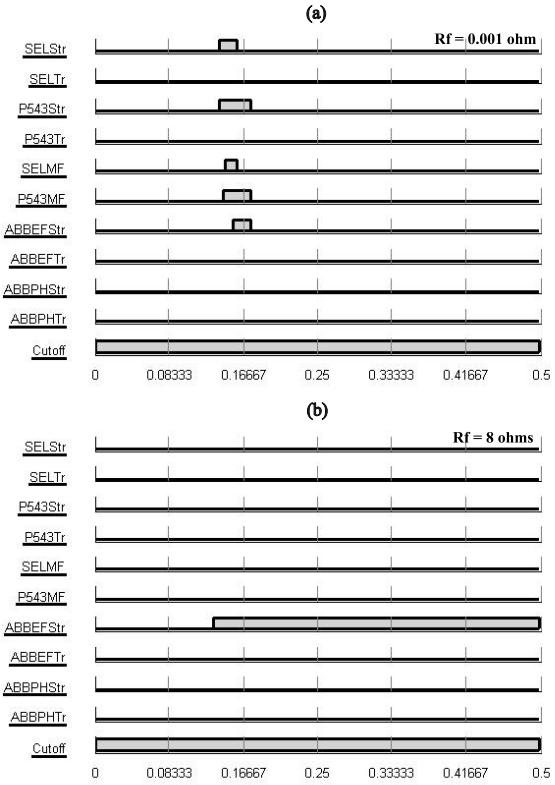

FIGURE 13. Test case 1. Detection of the AG MFF type at 25 km with fault resistance 0.001 Ohms (a) and 8 Ohms (b).

Moreover, Fig. 13 shows the starting and tripping signals sent from the three IEDs under test upon occurrence of an AG MFF type in the system at 25 km with $R_f = 0.001$ Ω (a) and $R_f = 8$ Ω (b). As it can be seen from Fig. 13a, the MFFPF is able to operate correctly with the two rOUTs, as seen for the "SELMF" and "P543MF" binary signals. In this case, only the relays at the faulted feeders operate to clear the MFF from the system, and the healthy outgoing feeders are continuously energized without interruption. This behaviour applies for all the parameter combinations leading to the "pass" interoperability verdict in Fig. 11. On the other hand, if $R_f = 8$ Ω, the MFFPF is unable to detect the AG MFF type when the fault is located 25 km away from the substation. In this case, the interoperability test fails, since the MFFPF cannot detect the high resistance MFF, and only rINC is able to detect MFF, as seen for the "ABBEFStr" binary signal of Fig. 13b. The same behavior is recorded for the BG and CG MFF fault types.

B. TEST CASE 2: ONLY ONE TRANSFORMER ENERGIZED ON BUS 2 WITHOUT DG CONNECTED

The network topology of this test case is the power system model of Fig. 10 with no DG connected, incoming 2 and tie CBs closed, and the incoming 1 CB open. This reflects the situation in which the power transformer connected to bus 1 cannot be energized or is under maintenance.

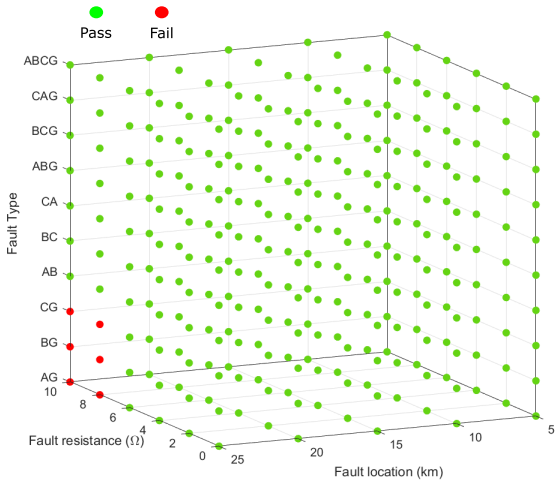

FIGURE 14. Test case 2. Interoperability verdict of rOUT1 of all fault types for different fault resistance values and fault locations. Same results are observed for rOUT2.

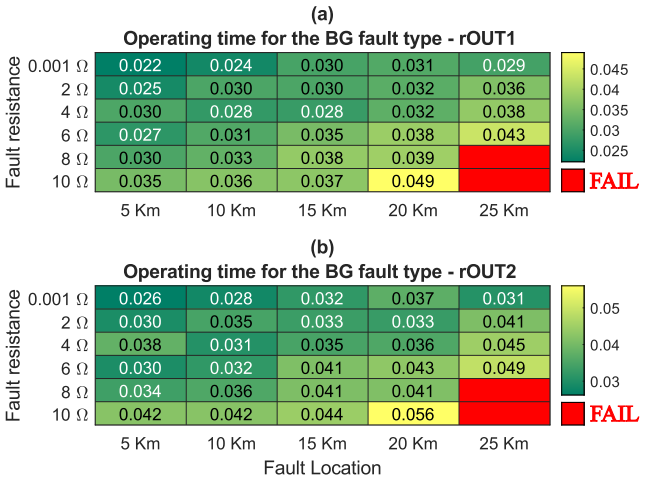

FIGURE 15. Test case 2. Operating times of rOUT1 and rOUT2 in the case of an BG MFF type for different fault resistance values and fault locations.

As shown in Fig. 14, the simulations performed with the parameter values of Table 5 reveal that, similarly to the test case 1, lack of interoperability (according to Eq. (8)) is recorded only for the fault types AG, BG and CG, with the others always leading to a "pass" interoperability verdict for any location and any MFF resistance value.

More details can be observed in Fig. 15, which shows the operating times of the MFFPF for the two IEDs in the case of an BG MFF type. As it can be seen, the MFFPF reveals to be interoperable for $R_f \leq 6\ \Omega$ regardless of the fault location. For values of $R_f \geq 8\ \Omega$, the MFFPF fails to detect BG MFF type for fault location of 25 km away from the substation. This behavior is recorded also for AB and CG MFF types. The same considerations done in test case 1 regarding the low probability of occurrence of single-phase-to-ground MFF and the operation of HIF function apply also here.

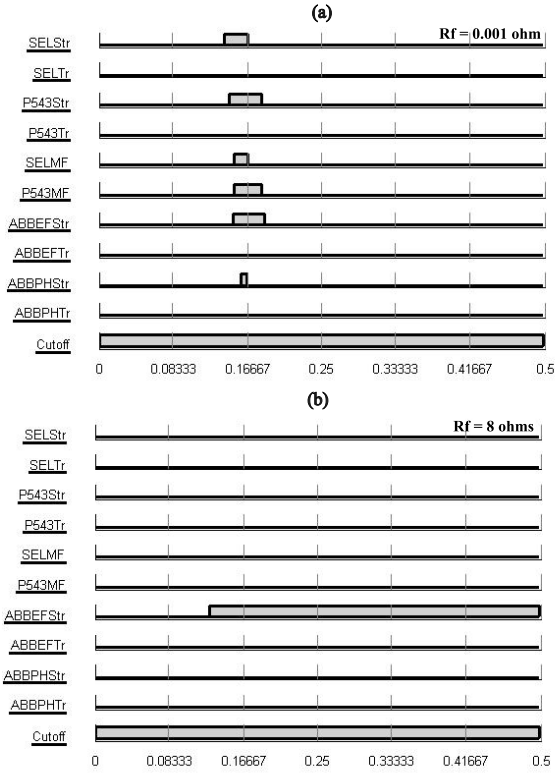

FIGURE 16. Test case 2. Detection of the BG MFF type at 25 km with fault resistance 0.001 Ohms (a) and 8 Ohms (b).

Fig. 16 shows the starting and tripping signals of IEDs once an BG MFF type occurs in the system at 25 km for $R_f = 0.001\ \Omega$ (a) and $R_f = 8\ \Omega$ (b). For $R_f = 0.001\ \Omega$, the MFFPF is able to deal with the MFF as indicated by the "SELMF" and "P543MF" signals of Fig. 16a. If $R_f = 8\ \Omega$, only rTB is able to detect the MFF, as represented by the "ABBEFStr" binary signal of Fig. 16b. The same MFF characteristic is recorded for the AG and CG MFF types. In this case, the rTB trips faster than rOUTs and leads all outgoing feeders connected to bus 1 to disconnect from the system.

C. TEST CASE 3: TWO TRANSFORMERS ENERGIZED WITH DG CONNECTED

The network topology of this test case is the power system model of Fig. 10 with DG connected to feeder 2 at 3 km away from the substation, both incoming CBs closed, and the tie CB open. The operation of the OCPF at the DG connection point is not considered, as the focus is only on the interoperability of the proposed scheme in presence of the in-feed effect of DG.

As shown in Fig. 17, the simulations performed with the parameter values of Table 5 reveal that lack of interoperability (according to Eq. (8)) is recorded only for the fault types AG, BG and CG, with the others always leading to a "pass" interoperability verdict for any location and any MFF resistance value.

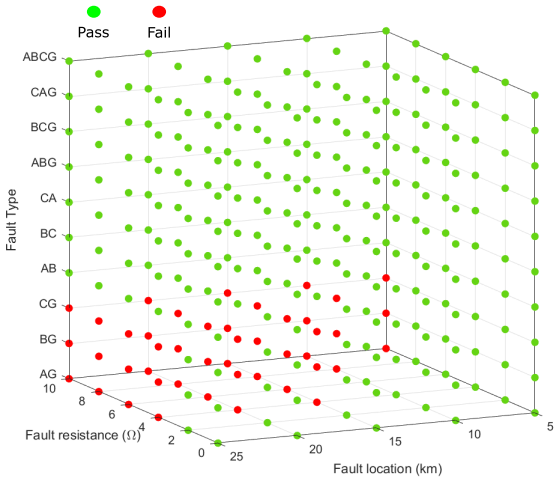

FIGURE 17. Test case 3. Interoperability verdict of rOUT1 of all fault types for different fault resistance values and fault locations. Same results are observed for rOUT2.

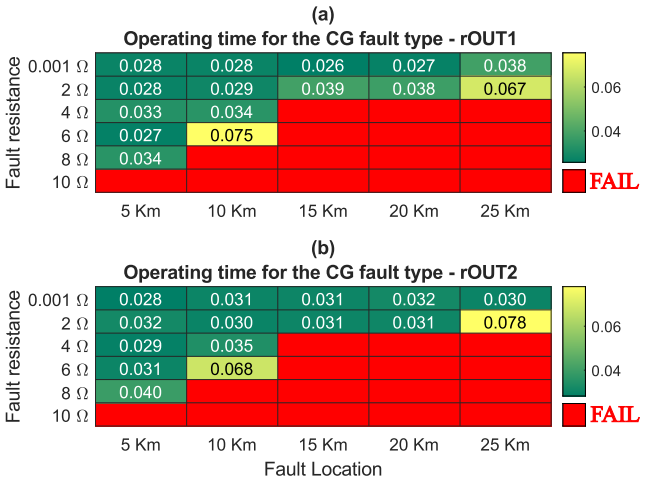

FIGURE 18. Test case 3. Operating times of rOUT1 and rOUT2 in the case of an CG MFF type for different fault resistance values and fault locations.

More details can be observed in Fig. 18, which shows the operating times of the MFFPF for the two IEDs in the case of an CG MFF type. As it can be seen, the region of non-interoperability is wider than that of test case 1 (Fig. 12) and 2 (Fig. 15), with "fail" interoperability verdict recorded already for $R_f \geq 4\ \Omega$ and fault location higher than 10 km. For $R_f \geq 10\ \Omega$, a "fail" interoperability verdict is obtained regardless of the fault location. The same behavior is recorded for the AG and BG MFF types. Such worsening of the interoperability of the MFFPF is due to the in-feed effect of DG, which directly impacts the current detection of rOUTs in the case of single-line-to-ground fault types. Overall, the connection of DG as well as the increase of R_f and fault location lead to a decrease in the protection zone of the rOUTs. Nonetheless, in these situations, HIF functions activate to deal with the MFF.

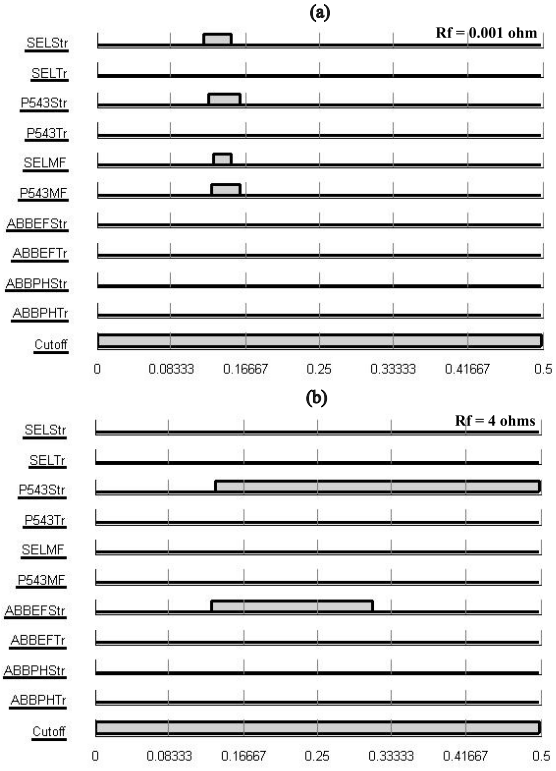

FIGURE 19. Test case 3. Detection of the CG MFF type at 15 km with fault resistance 0.001 Ohms (a) and 4 Ohms (b).

Moreover, Fig. 19 shows the starting and tripping signals sent from the three IEDs under test upon occurrence of an CG MFF type in the system at 15 km with $R_f = 0.001\ \Omega$ (a) and $R_f = 4\ \Omega$ (b). As it can be seen from Fig. 19a, the MFFPF is able to operate correctly for all fault types and locations with the two rOUTs. On the other hand, if $R_f = 4\ \Omega$, the MFFPF is unable to detect the CG MFF type when the fault is located 15 km away from the substation, since only rOUT1 and rINC can detect the MFF, as indicated by the "P543Str" and "ABBEFStr" signals of Fig. 19b. In other words, although the MFF occur in front of rOUT 1 and 2, only rOUT1 can detect the MFF. In this case, the rOUT1 operates to clear the fault based on the inverse time characteristic.

VIII. CONCLUSION

This paper proposes an IEC 61850 based protection scheme elaborated with the directional element using the GOOSE communication protocol in order to deal with the MFF in distribution systems. The proposed scheme can be implemented with the internal logic and programming within IEDs without any additional equipment installation, and fills the gaps of the existing OCPF in the presence of MFF.

In addition, a testing platform is developed to verify the interoperability between the proposed protection scheme and different (possibly multi-vendor) IEDs at the bay level of the digital substation. With the proposed testing platform, electricity utilities can validate the protection and control scheme according to their requirements to detect possible errors (e.g.,

due to the logical process, configurations, and parameter settings of the IEDs) before the field implementation.

The selected test cases elaborated to investigate all the switching operations and the effect of DG connection (without considering the OCPF at the DG connection point) illustrate that, in the case of multi-phase-to-ground and phase-to-phase MFF, the proposed scheme enhances the selectivity and reliability of the protection system at the digital substation by separating only the faulted feeders, while the healthy ones remain energized. This way, customers connected to the unfaulted feeders are continuously energized without interruption by MFF, ultimately leading to an increased customer service quality and availability, reduced outage costs, as well as improved network reliability. In other words and unlike the existing protection schemes applied for MFF, following the proposed protection scheme healthy feeders remain fully connected and energized to the system.

IX. DISCUSSION AND FUTURE WORK

For the case of not having DGs and for multi-phase-to-ground and phase-to-phase MFF, the proposed scheme reveals to be always interoperable. In the case of single-phase-to-ground MFF though, lack of interoperability has been highlighted for high values of fault resistance (e.g., greater than 8 Ω) and fault locations far away from the substation (e.g., 25 km). However, single-phase-to-ground MFF are less likely to happen than multi-phase-to-ground and phase-to-phase MFF, as MFF usually involve at least two conductors of two outgoing feeders: once the MFF occurs, the fault current is high enough for allowing the proposed scheme to detect the MFF. Moreover, it is noteworthy that high resistance faults might be dealt with by using a HIF function, which is normally available in commercial IEDs. Nonetheless, the capability of HIF technologies to mitigate the effect of high resistance fault must be properly verified and might be topic for further investigation.

For the case of having DGs and for multi-phase-to-ground and phase-to-phase MFF, the proposed scheme reveals to be always interoperable. However and for the single-phase-to-ground MFF, the non-interoperability region becomes wider when DG is connected to the distribution line (for fault resistance greater than 4 Ω and for fault locations relatively closer to the substation). Such worsening of the interoperability happens when the DG is connected quite close to the substation (as studied in this work), which represents a potential worst-case scenario for current detection in both directions (forward and reverse). Future work is envisaged to accurately investigate the sensitivity of the current detection of OCPF with respect to the in-feed effect of the DG for different locations and capacity, the MFF resistance, the MFF location and the MFF types.

REFERENCES

[1] P. Teansri, R. Bhasaputra, W. Pattaraprakorn, and P. Bhasaputra, "Outage cost of industries in Thailand by considering Thailand standard industrial classification," *GMSARN Int. J.*, vol. 4, nos. 1–5, pp. 37–48, 2010.

[2] L. Lawton, M. J. Sullivan, K. V. Liere, A. Katz, and J. H. Eto, "A framework and review of customer outage costs: Integration and analysis of electric utility outage cost surveys," Lawrence Berkeley Nat. Lab., Berkeley, CA, USA, Tech. Rep. 11/2003 2003.

[3] L. Kumpulainen, A. Jäntti, J. Rintala, and K. Kauhaniemi, "Benefits and performance of IEC 61850 generic object oriented substation event-based communication in arc protection," *IET Gener., Transmiss. Distrib.*, vol. 11, no. 2, pp. 456–463, Jan. 2017. [Online]. Available: https://ietresearch.onlinelibrary.wiley.com/doi/abs/10.1049/iet-gtd.2016.1003

[4] D. D. Giustina, A. Dedè, G. Invernizzi, D. P. Valle, F. Franzoni, A. Pegoiani, and L. Cremaschini, "Smart grid automation based on IEC 61850: An experimental characterization," *IEEE Trans. Instrum. Meas.*, vol. 64, no. 8, pp. 2055–2063, Aug. 2015.

[5] H. F. Habib, N. Fawzy, M. M. Esfahani, O. A. Mohammed, and S. Brahma, "An enhancement of protection strategy for distribution network using the communication protocols," *IEEE Trans. Ind. Appl.*, vol. 56, no. 2, pp. 1240–1249, Mar. 2020.

[6] V. Ferrari and Y. Lopes, "Dynamic adaptive protection based on IEC 61850," *IEEE Latin Amer. Trans.*, vol. 18, no. 7, pp. 1302–1310, Jul. 2020.

[7] M. Ghotbi-Maleki, R. M. Chabanloo, H. H. Zeineldin, and S. M. H. Miangafsheh, "Design of setting group-based overcurrent protection scheme for active distribution networks using MILP," *IEEE Trans. Smart Grid*, vol. 12, no. 2, pp. 1185–1193, Mar. 2021.

[8] J. B. Manuel, H. E. L. Zavala, E. A. Ramírez, D. S. Escobedo, and H. J. Altuve, "Protecting distribution feeders for simultaneous faults," in *Proc. 63rd Annu. Conf. Protective Relay Engineers*, Mar. 2010, pp. 1–9.

[9] Y. M. Nsaif, M. S. H. Lipu, A. Ayob, Y. Yusof, and A. Hussain, "Fault detection and protection schemes for distributed generation integrated to distribution network: Challenges and suggestions," *IEEE Access*, vol. 9, pp. 142693–142717, 2021.

[10] G. Manassero, E. L. Pellini, E. C. Senger, and R. M. Nakagomi, "IEC61850–based systems—Functional testing and interoperability issues," *IEEE Trans. Ind. Informat.*, vol. 9, no. 3, pp. 1436–1444, Aug. 2013.

[11] J.-C. Tan, V. Green, and J. Ciufo, "Testing IEC 61850 based multi-vendor substation automation systems for interoperability," in *Proc. IEEE/PES Power Syst. Conf. Expo.*, Mar. 2009, pp. 1–5.

[12] P. Zhang, L. Portillo, and M. Kezunovic, "Compatibility and interoperability evaluation for all-digital protection system through automatic application test," in *Proc. IEEE Power Eng. Soc. Gen. Meeting*, Jun. 2006, pp. 1–7.

[13] A. Rene and A. James, "Integration and testing challenges of IEC 61850 multivendor protection schemes," in *Proc. 10th IET Int. Conf. Develop. Power Syst. Protection (DPSP), Manag. Change*, 2010, pp. 1–5.

[14] T. Sidhu, M. Kanabar, and P. Parikh, "Configuration and performance testing of IEC 61850 GOOSE," in *Proc. Int. Conf. Adv. Power Syst. Autom. Protection*, vol. 2, Oct. 2011, pp. 1384–1389.

[15] Provincial Electricity Authority, "Substation control and protection system (SCPS)," Tech. Rep. RSUB-010/2560 (Rev. 1.0), 2017. Accessed: Jan. 4, 2023. [Online]. Available: https://www.pea.co.th/Webapplications/tor/Attachments/083e7e4b-2862-4a25-a88c-ae58c91fb34a/Specification%20No%20RSUB-0102560%20(Rev.1.0).pdf

[16] H. F. Habib, N. Fawzy, and S. Brahma, "Performance testing and assessment of protection scheme using real-time hardware-in-the-loop and IEC 61850 standard," *IEEE Trans. Ind. Appl.*, vol. 57, no. 5, pp. 4569–4578, Sep. 2021.

[17] Z. Yang, Y. Wang, L. Xing, B. Yin, and J. Tao, "Relay protection simulation and testing of online setting value modification based on RTDS," *IEEE Access*, vol. 8, pp. 4693–4699, 2020.

[18] A. Delavari, P. Brunelle, and C. F. Mugombozi, "Real-time modeling and testing of distance protection relay based on IEC 61850 protocol," *Can. J. Electr. Comput. Eng.*, vol. 43, no. 3, pp. 157–162, 2020.

[19] *Network Protection and Automation Guide*, Alstom Grid, Saint-Ouen-sur-Seine, France 2011.

[20] SEL. (2017). *Instruction Manual, SEL-751 Feeder Protection Relay*. Accessed: Jan. 13, 2023. [Online]. Available: https://sertecrelays.net/wp-content/uploads/2019/02/751_IM_20170927.pdf

[21] ABB. (2013). *Technical Manual, 615 Series*. Accessed: Jan. 13, 2023. [Online]. Available: https://library.e.abb.com/public/389adf763fb4f46ac1257c7b00438810/RE_615_tech_756887_ENg.pdf

[22] Schneider Electric. (2020). *Technical Manual, Easergy MiCOM P54x*. Accessed: Jan. 13, 2023. [Online]. Available: https://rza.by/upload/iblock/3c3/9ja3pb4ek7d6yv0mejf32tysrfskf5sk/P54x_EN_M_Vk5__K3__M.pdf

[23] *Communication Networks and Systems for Power Utility Automation—Part 10: Conformance Testing*, Standard IEC 61850-10:2012, International Standard, 2011.
[24] Y. Yuan and Y. Yang, *IEC61850-Based Smart Substations: Principles, Testing, Operation and Maintenance*. Amsterdam, The Netherlands: Elsevier, 2019.
[25] *Communication Networks and Systems for Power Utility Automation—Part 6: Configuration Description Language for Communication in Electrical Substations Related to IEDs*, Standard IEC 61850-6:2014, International Standard, 2009.
[26] H. Ferrer and E. Schweitzer, *Modern Solutions for Protection, Control, and Monitoring of Electric Power Systems*. Pullman, WA, USA: Schweitzer Engineering Laboratories, 2010.
[27] Omicron. (2022). *Voltage and Current Amplifier, CMS356 Brochure*. Accessed: Feb. 27, 2023. [Online]. Available: https://www.omicronenergy.com/en/products/cms-356/
[28] *Communication Networks and Systems for Power Utility Automation—Specific Communication Service Mapping (SCSM)—Mappings to MMS (ISO 9506-1 and ISO9506-2) and to ISO/IEC 8802-3*, Standard IEC 61850-8-1:2011, International Standard, 2011.
[29] W. Huang, "Learn IEC 61850 configuration in 30 minutes," in *Proc. 71st Annu. Conf. Protective Relay Eng. (CPRE)*, Mar. 2018, pp. 1–5.
[30] *Criteria Setting of Protection Functions in Transmission and Distribution System*, Provincial Electr. Authority Thailand, Bangkok, Thailand, 2009.

THANAKORN PENTHONG received the M.Eng. degree in electrical power engineering from Kasetsart University, Bangkok, Thailand, in 2013. He has been working for PEA in the power system control and protection division, since 2010. He is currently a Research Assistant with the Institute for Automation of Complex Power Systems, E.ON Energy Research Center, RWTH Aachen University. His current research interests include power system protection, monitoring, and control.

MIRKO GINOCCHI (Member, IEEE) received the M.Sc. degree in sciences and technology for environment and landscape from the University of Milano-Bicocca, Milan, Italy, in 2014. He joined the Sensitivity Analysis of Model Output Group, Competence Centre on Modelling, and the European Commission Joint Research Centre, Ispra, Italy, in 2016. He joined the Institute for Automation of Complex Power Systems, E.ON Energy Research Center, RWTH Aachen University, Aachen, Germany, in 2018, where he is currently a Research Assistant. His research interests include uncertainty and sensitivity analysis for power system applications, interoperability testing for smart grids, and the statistical design of laboratory experiments.

AMIR AHMADIFAR (Member, IEEE) received the M.Sc. degree in electrical engineering, information technology, and computer engineering from RWTH Aachen University, Aachen, Germany, in 2017. He is currently a Research Associate with the E.ON Energy Research Center, Institute for Automation of Complex Power Systems, RWTH Aachen University. His current research interests include power system modeling, analysis, control, the smart management of active distribution grids, and renewable energies integration in smart grids with high levels of electric mobility.

FERDINANDA PONCI (Senior Member, IEEE) received the Ph.D. degree in electrical engineering from Politecnico di Milano, Italy, in 2002. She joined the Department of Electrical Engineering, University of South Carolina, Columbia, SC, USA, as an Assistant Professor, in 2003, and was a tenured promoted, in 2008. In 2009, she joined the E.ON Research Center, Institute for Automation of Complex Power Systems, RWTH Aachen University, Aachen, Germany, where she is currently a Professor in monitoring and distributed control for power systems. Her research interests include advanced measurement, monitoring, and the automation of active distribution systems. She is an elected member of the Administration Committee of the IEEE Instrumentation and Measurement Society and the Liaison with IEEE Women in Engineering.

ANTONELLO MONTI (Senior Member, IEEE) received the M.Sc. degree (summa cum laude) and the Ph.D. degree in electrical engineering from Politecnico di Milano, Italy, in 1989 and 1994, respectively. He started his career with Ansaldo Industria and then moved to Politecnico di Milano, as an Assistant Professor, in 1995. In 2000, he joined the Department of Electrical Engineering, University of South Carolina (USA), as an Associate and then a Full Professor. Since 2008, he has been the Director of the E.ON Energy Research Center, Institute for Automation of Complex Power System, RWTH Aachen University. Since 2019, he holds a double appointment with Fraunhofer FIT, where he is currently developing the new Center for Digital Energy, Aachen. He is the author or coauthor of more than 400 peer-reviewed papers published in international journals and in the proceedings of international conferences. He is an Associate Editor of *IEEE Electrification Magazine*, a member of the editorial board of the *SEGAN* journal (Elsevier), and a member of the Founding Board of the *Energy Informatics* journal (Springer). He was a recipient of the 2017 IEEE Innovation in Societal Infrastructure Award.